Journal of Nuclear Materials 381 (2008) 83–91

Contents lists available at ScienceDirect

Journal of Nuclear Materials

journal homepage: www.elsevier.com/locate/jnucmat

Application of an independent parallel reactions model on the annealing kinetics to irradiated graphite waste

Michael Lasithiotakis [a,b,*,1], Barry Marsden [a,b,1], James Marrow [a,b,1], Andrew Willets [a]

[a] Materials Performance Centre, School of Materials, The University of Manchester, P.O. Box 88, Manchester M60 1QD, UK
[b] Nuclear Graphite Research Group (NGRG), School of Mechanical, Aerospace and Civil Engineering, The University of Manchester, P.O. Box 88, Manchester M60 1QD, UK

ARTICLE INFO

Keywords:
Graphite
Irradiation
Kinetics
Annealing
Activation energy

ABSTRACT

The first generation of UK research and production reactors were graphite moderated and operated at low temperatures, below 150 °C. The graphite in these reactors now contains a significant amount of stored (Wigner) energy that may be relatively easily released by heating the graphite above the irradiation temperature. This exothermic behaviour has lead to a number of decommissioning issues which are related to characterization of graphite samples, long term "safe-storage", reactor core dismantling, graphite waste packaging and the final disposal of this irradiated graphite waste. The release of stored energy can be modelled using kinetic models linked to classical kinetic analysis theory. These models rely on Differential Scanning Calorimeter (DSC) data obtained either from graphite samples irradiated in material test reactors or data obtained from small samples trepanned from the reactors themselves. Data from these experiments can be used to derive activation energies and characteristic functions used in kinetic models for application to practical situations using suitable modelling techniques. In this paper the classical theory of kinetic analysis is used as the basis for models applied to the study of stored energy release in irradiated graphite components. The use of an independent parallel reactions model is proposed and several possible kinetic model scenarios are tested.

1. Introduction

Graphite has been used since the 1940s as a moderator and structural material in the cores of fission reactors and has therefore been exposed to fast neutron irradiation under various conditions at a variety of irradiation temperatures. In graphite irradiated at a low temperature, i.e. below 150 °C, an important phenomenon caused by the neutron damage to the graphite is the potential release of stored energy when heated around 200 °C. This is well known as Wigner energy release. As Wigner energy is correlated with other irradiation induced property changes in graphite the elucidation of the mechanism of Wigner energy release is also important in the understanding and interpretation of the other radiation damage phenomena in graphite at these low temperatures.

Many measurements of Wigner energy release have been undertaken [1–6], mostly, before the advent of modern computational facilities for data analysis. These were aimed at assessing the parameters of the annealing process in reactors operating at low temperatures (i.e. to determine the activation energy E_a and pre-exponential factor A in the Arrhenius equation). Some of these analyses consider the annealing procedure as a one stage reaction [1,2] and some very simple models have been applied in an effort to simulate experimental Differential Scanning Calorimetry (DSC) data obtained from irradiated graphite samples [1,2,4,5]. A common problem in these early models was their simplicity and the assumptions necessarily made due to the absence of computational power, which prohibited previous researchers from applying more complicated models that should be capable of deriving more realistic results. Furthermore, the kinetics of stored energy release is *a priori* complex because the measured energy release spectra are observed to be too broad to be analysed by a single activated process.

What should be expected from a rigorous kinetic model depends on the purpose of the investigation and on the particular properties of the irradiated samples. For example, a description of the behaviour of the samples over a wide range of experimental conditions is required in order to have confidence in the ability to predict the behaviour outside the domain of experimental investigation. Such a wide database can be used to establish a deeper insight into the processes involved.

The kinetics of Wigner energy release can provide a better understanding of radiation damage in graphite and a robust prediction of stored energy release, particularly for new conditions

* Corresponding author. Address: Materials Performance Centre, School of Materials, The University of Manchester, P.O. Box 88, Manchester M60 1QD, UK. Tel.: +44 (0) 161 306 4840; fax: +44 (0) 161 306 4865.
E-mail address: Michael.Lasithiotakis@postgrad.manchester.ac.uk (M. Lasithiotakis).
[1] Tel.: +44 (0) 161 275 4399.

0022-3115/$ - see front matter © 2008 Elsevier B.V. All rights reserved.
doi:10.1016/j.jnucmat.2008.07.039

outside the scope of present understanding, such as for decommissioning purposes. Kinetic analysis is a useful tool for gaining an understanding of the characteristics of the annealing procedures-reactions especially if it can be correlated with microstructural analysis using techniques such as Transition Electron Microscope and Raman Spectroscopy. In the future it is also proposed to test these various kinetic models against new experimental data.

In this paper, historic measurements and early kinetic analysis of the stored energy release spectra in neutron irradiated graphite have been investigated. Data for a series of historical experiments on different types of graphite with relatively different DSC profiles has been reanalyzed. Classical theory of kinetic analysis developed over a number of years has been applied using new more complex validated models, which are more suitable for the study of stored energy. The use of this more sophisticated modelling, accounts for proposed independent parallel reactions. Various possible kinetic scenarios are tested.

2. Experimental conditions of historic data

2.1. Experimental data have been taken from the following sources

Simmons [2] gives data from two specimens of graphite taken from the Windscale piles, one sample with a fast neutron fluence of 9.0×10^{20} n/cm^2 Equivalent Dido Nickel Dose (EDND) at a irradiation temperature of 95 °C, and one sample with a fluence of 3.0×10^{20} n/cm^2 EDND with an irradiation temperature of 76 °C. The DSC profiles of this series are shown in Fig. 1, as a plot of the time derivative of the normalized energy (divided by the final energy produced S_f or $S_{inf,}$ depending on whether there was an isothermal stage at the end of the experiment) released versus temperature. For the kinetic assessments Simmons used three models, the Constant Activation Energy Model, the General Model and the Constant Frequency/Variable Energy Model. The first model is based on the assumption that Activation energy remains constant over the temperature range of the release. The General Model assumes that Activation Energy is a function of temperature, and the Constant Frequency/Variable Energy Model assumes a dependence of activation energy through the mathematical relationship:

$$v \int_0^t \exp\left[-\frac{E_0}{kT(t)}\right] dt = 1, \quad (1)$$

where v is the frequency, E_0 is the activation energy, k is Boltzmann's constant and $T(t)$ is the temperature as a function of time. The DSC experiments reported were at heating rates of 2.5, 25, and 50 °C/min. The Windscale data from Simmons shows a peak in the rate of release curve around 200 °C. He then assumed activation energy of between 1.2 eV and 2.0 eV for all three models. All three models used showed little or moderate convergence with the experimental data.

Preston et al. [1] obtained data from seven specimens also originating from the Windscale Piles. Little is known of the irradiation history of the specimens, other than that they were taken from graphite dowels recovered from the air inlet ducts of Windscale Piles 1 and 2. Three dowels were sent from Pile 1 (Building B2) and four dowels from Pile 2 (Building B12). Each dowel was approximately 4 cm diameter by 30 cm long. The rate of release data was obtained by Preston at the Chapelcross graphite laboratory as follows. Specimens 7 mm diameter by 2 mm thick (weighing around 100 mg) were cored from the end of each dowel. The samples were denoted by the building number, dowel number and the end of the dowel from which the sample had been cut, e.g. B12/2L for building B12, second dowel, left end, and the same codes are followed by this paper. The rate of release of stored energy was measured over the temperature range 40–500 °C. Heating rates were 10 °C/min for all DSC runs. The samples were held for one hour at 500 °C between the annealing run and the subsequent run to ensure that all the stored energy had been released up to this temperature. During the test the sample containers were continually purged with high purity argon to prevent oxidation. The Preston data series exhibits peak shapes of the same form as the earlier Simmons series, which maybe expected since all of these specimens originated from the Windscale piles. The peak rate of release also appears at a similar temperature of around 200 °C. The DSC profiles from Preston's experiments are shown by Fig. 2, and are a plot of the time derivative of the normalized energy released versus temperature.

Lexa et al. [3] used specimens obtained from the ASTRA research reactor thermal column (ASTRA was a 10 MW light water moderated and cooled pool type research reactor in Seibersdorf, Austria). Each specimen was sampled from the pyramidal inner thermal column by core drilling at seven positions along the column's longitudinal axis labelled a–g, at distances from the surface near the reactor core ranging from 0.0 to 0.6 m. Five DSC samples from each position were machined: three simple disks, 8.0 mm in diameter and 1.0 mm thick, weighing approximately 80 mg, for differential scanning calorimetry, and two two-layer 'wedding-cake' shaped disks, with an 8.0×0.5 mm base and a 6.0×0.5 mm top, weighing around 65 mg. The samples were machined on a lathe at reduced speed with alcohol cooling in order that that the temperature did not exceeded 25 °C. This was in order to prevent Wigner energy release). The heating rate was 10 °C/min

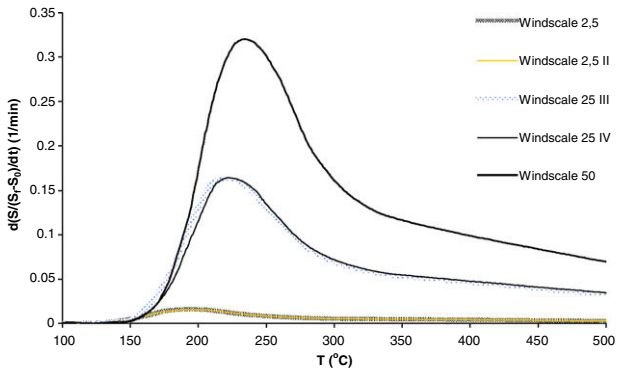

Fig. 1. The series of the Windscale DSC data due to Simmons [2], giving the rate of normalized energy released (S/S_{inf}) versus temperature for all 5 different DSC curves. The heating rate range varied from 2, 5 to 50 °C/min as shown by the numbers in the legend. The peak temperature is around 200 °C.

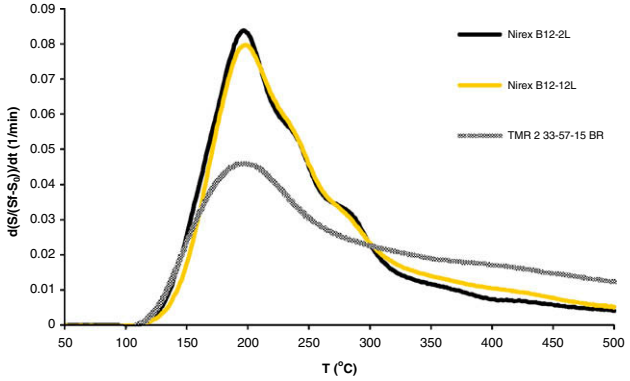

Fig. 2. The series of three DSC data [1] due to Preston (Nirex industrial report [1]). The rate of normalized energy released (S/S_{inf}) versus temperature is shown. The shape of the peaks has the same form with the Simmons series. The heating rate was 10 °C/min for all three experiments. The peak temperature is also around 200 °C.

for all experiments. The DSC profiles of this series are shown in Fig. 3, as a plot of the time derivative of the normalized energy released versus temperature. The Lexa series of data is encoded here as 'Lexa a' to 'Lexa g'. The shape of the 'Lexa a' to 'Lexa e' peaks is of a similar form to the Simmons and Preston Windscale samples with a 200 °C peak. However, the Lexa f and Lexa g DSC series have a different shape.

Iwata et al. [4] used pyrolytic graphite samples, heat-treated at 3000 °C in a Freon gas atmosphere. His specimens were neutron-irradiated at 80 °C to an approximate fluence of 4×10^{17} n/cm^2 ($E > 1$ MeV) in the JAERI JRR-2 experimental reactor. Displacements per atom (dpa) were estimated to be 6–8 $\times$ 10^{-4}. Stored energy release spectra were measured at constant rates of heating in a nitrogen gas atmosphere using the DuPont 910 Differential Scanning Calorimeter. Heating rates were 1, 2, 5, 10, 20, 50 and l00 °C/min.

The series of the Iwata DSC data have relatively different shapes for the higher heating rates. The shape of the peaks is different from the Simmons and Preston data. There is a peak at temperatures less than 200 °C but it is moving towards higher values of temperature as a function of heating rate. The DSC profiles of this series are shown in Fig. 4 as a plot of the time derivative of the normalized energy released versus temperature.

3. Kinetic model

The thermal annealing of graphite is understood through the use of kinetic models. Mathematical models are first developed and their parameters fitted to data from a DSC analysis.

The basic relation from which all the kinetic approaches begin is the following [2,4–9]:

$$\frac{dx}{dt} = kf(x), \tag{2}$$

where x is a variable that follows the Arrhenius distribution with linear increase of time, $f(x)$ is a mathematical function of x, which characterizes the sample, and k is the constant of proportionality. In the annealing kinetics of Wigner energy release $x = S$, where S is the energy released during the linear increase of temperature in a DSC experiment. Various forms of the functions $f(x)$ have been considered, such as $f(x) = x$, which is the simplest, the function $f(x) = x^n$ is used to consider a reaction of nth order, and the most complex is, $f(x) = x^n\ (1-qx)^m$ [10]. In addition variations of these have been consider, e.g. Prout and Tompkins [9] where $f(x) = x(1-x)$ with $n, q, m = 1$. In the annealing kinetics of graphite, it has been generally assumed by previous researchers [1,2,4] that a first degree equation of form $f(x) = x$ or $f(S) = S$ can be used to reasonably simulate the process and in general this has been preferred for the interpretation of the data due to its simplicity. Despite these possibilities, there have been few attempts [5] at applying the non-first degree models of the form of $f(S) = S^n$, which are described in this paper.

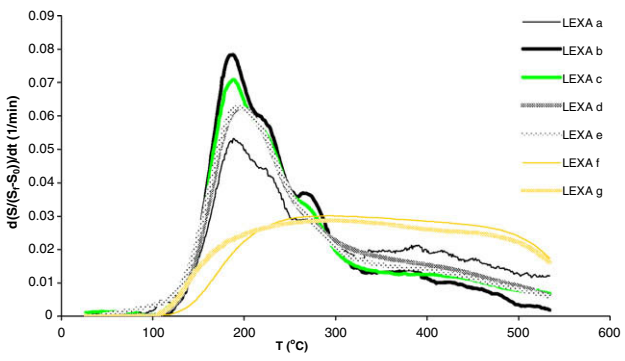

Fig. 3. The series of the Lexa DSC data [3]. The heating rate for all the experiments was 10 °C/min. The shape of the peaks has the same form as the Simmons and Preston series, except for the the Lexa f and Lexa g DSC series. The peak temperature in the Lexa a to Lexa e is around 200 °C.

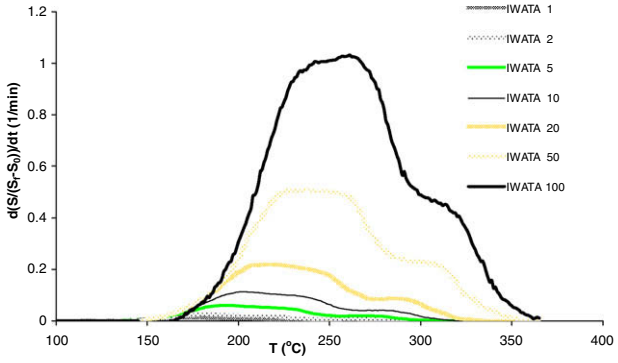

Fig. 4. The series of the Iwata DSC data [4]. The shape of the peaks appears slightly different from the Simmons and Preston series. The peak temperature moves towards higher values with increasing heating rate. The heating rate (°C/min is given by the numbers in the legend.

The objective of these methods is to assess the activation energy E_a, and pre-exponential factor or factor of Arrhenius A, for each process as expressed in the form of a standard Arrhenius equation:

$$k = A\exp\left(\frac{-E_a}{RT}\right), \tag{3}$$

or

$$k = A\exp\left(\frac{-E_a}{KT}\right), \tag{4}$$

where k is the factor of rate of reaction (specific rate); A, the Arrhenius factor or pre-exponential factor, or frequency factor; E_a, energy of activation, expressed in Joule/mol or Kev/molecule; R, the Universal Constant of Ideal Gases; k, the Boltzmann constant and T is the Absolute temperature. The above equation via natural logarithms gives:

$$\ln k = \ln A - \frac{E_a}{R}\frac{1}{T} \tag{5}$$

and

$$\log k = \log A - \frac{E_a}{2.303R}\frac{1}{T}. \tag{6}$$

From this equation we observe that the logarithm of the speed constant of reaction (k) is a linear function of the inverse absolute temperature $1/T$ with gradient equal to $-E_a/2.303R$ and intercept equal to the logarithm of pre-exponential or frequency factor. The gradient of this straight line is directly proportional to the activation energy (E_a). This linear equation can be easily fitted to the experimental measurements using the method of least squares.

4. The initial kinetic model

An initial attempt was made to assess activation energies, based on the model proposed by Simmons [2]. Constant activation energy – constant frequency model was assumed. Based on this assumption a simple equation for the rate of release of energy was used, as given below

$$\frac{dS}{dt} = A\exp\left(-\frac{E_a}{kT}\right)S. \tag{7}$$

This model has also been used by other researchers [1,4]. However the results of this assessment are strongly dependent on the user's choice of activation energy.

As previously discussed, Nightingale [5] used the following expression to describe the sharply peaked results he obtained.

$$\frac{dS}{dt} = A \exp\left(-\frac{E_a}{kT}\right) S^{\gamma}, \tag{8}$$

where γ was found to be in the ranges 6–8.

In Table 1, results from the kinetic approaches of two of the previous researchers [2,4] are given. Simmons predicted an activation energy of 116 KJ/mol for the constant energy model, and between 116 and 193 for the general model. Iwata reported three predominant reactions which he assumed as first order and with activation energies of 130, 145 and 172 KJ/mol, respectively. The pre-exponential factors calculated were 3.7×10^{10}, 1.4×10^{11} and 2.5×10^{12} (1/min). However, the comparison of the reconstructed overall calculated DSC curve with the experimental gave a poor fit.

An application of a kinetic model can be considered to be valid when the calculated kinetic model results converge with the experimental data. The above two models have been used to fit the experimental data available from the literature by several authors [2,4,5]. Both the models above have been used in this paper to determine the activation energy and pre-exponential factor. The modified Simmons model proved unsuccessful, with little resemblance between the experimental and predicted curves. The Nightingale model gave better comparisons but there were still significant differences.

In Figs. 5 and 6 the application of the above two models is shown. The figures show the plot of time derivative of the normalized energy released versus temperature. The Simmons model fails to reproduce the experimental curve. The Nightingale model gives better convergence, however it was still considered not adequate, since the shape of reconstructed curve fails to closely follow the shape of the experimental curve.

Considering the above model results, the need for a more complex model capable of interpreting the experimental DSC data emerged. This was achieved by the use of an independent parallel reactions model.

5. The independent parallel reactions model

The independent parallel reactions model has been used by researchers to study the chemical kinetics of heterogeneous reactions in fossil fuels [6,7,10-13]. This model presupposes the existence of independent parallel reactions taking place without interactions between them. For the kinetic analysis we can assume that the independent parallel reactions, also called partial reactions or 'pseudo-reactions', take place sequentially implying that a pseudo-reaction begin when the other finishes, or in parallel, supposing that pseudo-reactions develop simultaneously, without interaction with the others. Combinations of these two possibilities can also be selected, sequentially in some regions and in parallel in others.

Then the total production of energy and the rate of energy production for N overall reactions can be described as

$$S = \sum_i S_{i,t} \quad i = 1, 2, 3, \ldots, N, \tag{9}$$

$$\frac{dS}{dt} = \sum_i c_i \frac{ds_{i,t}}{dt}. \tag{10}$$

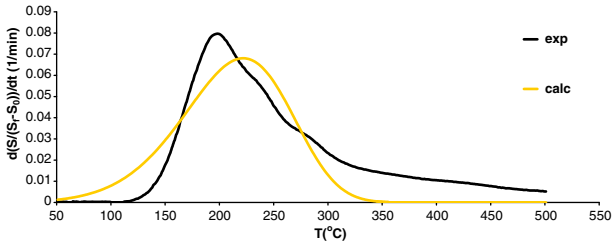

Fig. 5. Application of the Constant activation energy – Constant frequency model proposed by Simmons [2] to the experimental DSC curve Preston B12-2L. The experimental curve is depicted in black and the predicted in yellow. (For interpretation of the references to colour in this figure legend, the reader is referred to the web version of this article.)

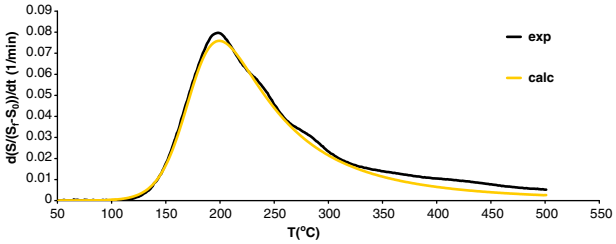

Fig. 6. Application of the Nightingale model [5] to the experimental DSC curve of Preston B12-2L. The experimental curve is depicted in black and the predicted in yellow. (For interpretation of the references to colour in this figure legend, the reader is referred to the web version of this article.)

The factor c_i accounts for the contribution of partial reactions i in the total energy produced $S_f - S_o$

$$c_i = S_{f,i} - S_{o,i}. \tag{11}$$

The fraction S_i that has released, for each component is given by

$$s_i = \frac{S_{f,i} - S_{i,t}}{S_{f,i} - S_{o,i}} \tag{12}$$

where $S_{f,i}$, $S_{i,t}$ and $S_{o,i}$, are the final energy released, energy released at time t (or temperature T), and the initial released energy, respectively (assuming initial released energy non zero). The components are assumed to decompose separately releasing a separate amount of energy to the overall energy content, according to the equation of Arrhenius:

$$\frac{ds_{i,t}}{dt} = A_i \exp\left(\frac{Ea_i}{RT}\right) s_{i,t}^{n}, \tag{13}$$

R is the universal gas constant, equal with $R = 8.314472$ J/(mol. °K). In this case the order of reaction n was considered equal to unity for the all reactions.

6. Calculation of kinetic parameters

For the analysis of DSC curves, (in the example below a first order reaction model is assumed), initial values of E_a, A and c, are

Table 1
Activation Energy and Pre-exponential factors as calculated by Iwata [4] and by Simmons [2]

Iwata [4]	n	A (1/min)	E_a (kJ/mol)	n	A (1/min)	E_a (kJ/mol)	N	A (1/min)	E_a (kJ/mol)
	1	3.7×10^{10}	130	1	1.42×10^{11}	145	1	2.5×10^{12}	172
Simmons [2]	Constant Activation Energy Model		116	General Model		116–193			

required for each of the pseudo-reactions. These are determined at step 1 in the following process [7,10–13]:

Step 1. Examine the DSC profiles and isolate regions of peaks, or shoulders. These regions are considered as regions where a partial reaction dominates above all the others. It is assumed for this region that the only reaction taking place is the particular reaction under consideration with no contribution from the others and consequently $S_{i,t} = S$. Rearranging the Arrhenius equation:

$$\frac{dS}{dt} = c\frac{ds_{i,t}}{dt} = (S - S_0)A_i \exp\left(-\frac{Ea_i}{RT}\right), \tag{14}$$

as

$$\frac{-\frac{dS}{dt}}{S - S_0} = c\frac{ds_i, t}{dt} = A_i \exp\left(-\frac{Ea_i}{RT}\right) \tag{15}$$

and by taking logarithms of the two parts of the equation:

$$\ln\left(\frac{-\frac{dS}{dt}}{S - S_0}\right) = \ln A_i - \frac{Eai}{RT}. \tag{16}$$

The above equation is a polynomial of the first degree, of the type $y = a + bx$, equating y with $\ln[-dS/dt/(S-S_0)]$ and x with $1/T$. Then the intercept a is $\ln(A)$ and the gradient b is $-Ea_i/R$. A least squares method is applied for the region containing the peak or the shoulder and a and b are calculated, leading to values for A and E_a. The values of A and E obtained, are considered to correspond only to the partial reaction that is assumed to be the only one occurring in this specific region.

The same procedure is applied for the all regions where shoulders or peaks have been observed. In this way E and A are determined for every single one of the regions studied.

Step 2. Certain reactions are added in order to reconstruct the overall DSC curve. The synthesis of the DSC curve is then compared with the experimental results. The curve is constructed as below:

$$\left[\frac{dS}{dt}\right]^{calc} = \sum_i c_i \frac{ds_{i,t}}{dt}, \tag{17}$$

where:

$$s_{i,t} = 1 - \exp\left[A_i/\beta \int_{To}^{T} \exp\left(-\frac{Ea_i}{RT}\right)dT\right] \tag{18}$$

and

$$\frac{ds_{i,t}}{dt} = A_i \exp\left(\frac{-Ea_i}{RT}\right)(s_{i,t}), \tag{19}$$

where β is the heating rate. The integral $\int_{To}^{T} \exp\left(-\frac{Ea_i}{RT}\right)dT$ is calculated numerically.

Step 3. A non-linear optimization algorithm is applied in order to achieve good convergence between experimental and calculated values. In the first step it is assumed that in the region of interest the partial reaction that dominates is unique, i.e. the only one taking place. But this assumption is obviously not realistic. There will be many cases, where two or more reactions are taking place almost at the same time, or other cases where partial overlapping of certain reactions are taking place. The result of this simplification is that the initial experimental DSC curve almost never coincides with calculated curve.

The divergence between calculated and experimental results is expressed as a percentage, associating the largest rate of reaction observed in experimental DSC curve, of the following type:

$$Dev1(\%) = 100\frac{\sqrt{SUM_{DSC}/(Z - Q)}}{\max[(-dS/dt)^{exp}]}, \tag{20}$$

where Z the total number of measurements that were used to represent the DSC curve and Q is the number of parameters that were used in the model, i.e. A, c and possibly n.The parameter SUM_{DSC} can be described as:

$$SUM_{DSC} = \sum_{z=1}^{Z}\left[\left(\left(\frac{dS_i}{dt}\right)^{exp}\right) - \left(\left(\frac{dS_i}{dt}\right)^{calc}\right)\right]^2. \tag{21}$$

The divergence between the experimental and calculated values of S_f is of the form:

$$Dev2\ (\%) = 100.abs\left[\frac{(S_f)^{exp} - (S_f)^{calc}}{(S_f)^{exp}}\right]. \tag{22}$$

The optimization of parameters *Dev1* and *Dev2* is achieved by use of a non-linear optimization algorithm. Because of the non-linearity of the problem, the algorithm can locate more than one solution. Consequently, particular care has to be applied in the choice of initial values, so that convergence to an appropriate solution is ensured.

7. Results and discussion

The following guidelines [6–13] have been applied to both the kinetic analysis and the independent parallel reactions model, to assess the accuracy of the models:

- Results are generally considered satisfactory when *Dev1* is less than 3%. As the parameters *Dev1* and *Dev 2* do not converge simultaneously, there has to be a choice between *Dev1* and *Dev 2*. It is therefore *Dev 1* which is usually chosen.
- A model is considered valid when application of the calculated model to experimental data other than that used in the fitting takes place, for verification. If a calculated model fits another series of experimental data, then it is considered as valid.
- In general the simplest model available is chosen. Simple models with few reactions are usually more durable when applied to different experimental data.
- Results between different experiments may vary slightly. It is considered essential is to produce results of the same order.
- The experimental conditions can make a significant difference to the variation in the experimental data. These might be heating rate, mass of sample, shape and condition of sample (solid or in powder form) etc.
- The shape of the predicted curve must follow the experimental shape. Even when the target of *Dev1* < 3% is achieved, the shapes of experimental and calculated curves can still be significantly different.
- The method depends on the experience of the analyst in choosing peaks and shoulders as a peak or a shoulder may not be so obvious.

The application of the Independent Parallel Reactions Model to stored energy release, due to it is complexity, can provide interpretations of various scenarios. Therefore it is important to validate the model against extensive experimental data.

Three different models have been tested. A model proposed by Simmons with six pseudo-reactions, a model proposed by Nightingale with six pseudo-reactions, and a third model proposed by Nightingale with five pseudo-reactions. The main difference between the first two models $f(S) = S$ (Simmons – 6 reactions) and the model $f(S) = S^n$ (Nightingale – 6 reactions) is that the parameter n, indicating the order of the annealing reaction is kept constant in the $f(S) = S$ (Simmons – 6 reactions) model, but is allowed to evolve during the optimization stage in the $f(S) = S^n$ (Nightingale – 6 reactions), thus these two models are related in so much as in the first model n is kept to unity and in the second model n is determined as one of the variables. The model on which the $f(S) = S^n$ (Nightingale –

5 reactions) is constructed is based on the assumption that there is one dominant annealing reaction taking place and there are four other reactions contributing into filling the gap between the dominant reaction and the experimental curve. This dominant reaction is defined by a fixed first-reaction, with pre-exponential factor of $A = 7.04 \times 10^{10}$ allowing the other parameters to be calculated by the algorithm. The above value was calculated by attempting to simulate the experimental curve with only one reaction, neglecting all the other partial reactions. Then, four other partial reactions were added considering the shoulders in the experimental curve after the 200 °C peak. The main concept behind the assumption in the latter model is that since there is a wide dominant peak around 200 °C for almost all the experiments, this must be the main annealing reaction taking place. For this reason a good model could be fitted using only 5 reactions instead of 6 as in the previous two models. For example, in Fig. 7 the DSC profile of the Iwata 5 experimental curve is compared with the predicted curve, together with the pseudo reactions contributing to the calculated curve. The DSC profiles are a plot of the time derivative of the normalized energy release versus time. The rate of heating was 5 °C/min. The type of model applied is the $f(S) = S$ (Simmons – 6 reactions). Reactions 4, 5, 6 participate with a percentage of less than 1% and therefore are not shown clearly in the diagram. The *Dev1* for this attempt was 6.75% which is considered to be unsatisfactory.

In Fig. 8 the DSC profile of the Preston specimen B2-2L is shown. The DSC profile of the experimental curve and the predicted curve along with the pseudo reactions used to construct the predicted curve are shown. The DSC profiles are a plot of the time derivative of the normalized energy released versus time. The rate of heating in this case was 10 °C/min. The type of model used for interpreting the annealing process was the $f(S) = S$ (Simmons – 6 reactions). The convergence between experimental and calculated values is relatively good, around 1.78%. The shape of the calculated curve follows the experimental results.

In Fig. 9 the DSC profile of the bulk specimen Iwata 1 is shown. The rate of heating in this case was 5 °C/min. The type of model fitted is $f(S) = S^n$ (Nightingale – 6 reactions). The application of $f(S) = S^n$ (Nightingale – 6 reactions) model gave better results for all specimens, in comparison to the $f(S) = S$ (Simmons – 6 Reactions) model.

In Fig. 10 the DSC profile of Preston specimen B12-2L, is shown. The DSC profile of the experimental curve is compared with the calculated curve, along with the pseudo reactions used to construct the calculated curve. The DSC profiles are a plot of the time derivative of the normalized energy released versus time. The rate of heating in this case was 10 °C/min. The type of model was $f(S) = S^n$ (Nightingale – 5 reactions). Excellent convergence is obtained between experimental and predicted curve and the shape of the calculated curve closely follows the experimental curve.

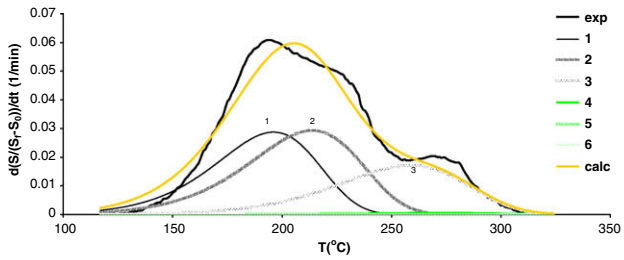

Fig. 7. Example of kinetic model (calc) fitting to experimental data (exp) for specimen Iwata 5, (rate of heating 5 °C/min) using the Simmons model with 6 pseudo-reactions. Reactions 4, 5, 6 participate with a percentage less than 1% and therefore sit on the *x*-axis.

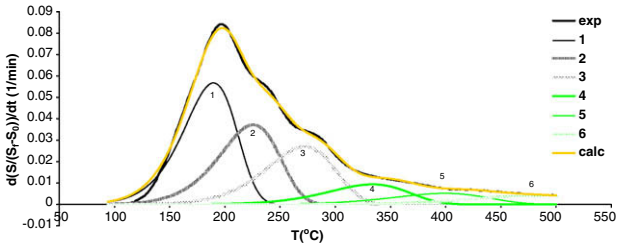

Fig. 8. Example of model fitting (calc) to data (exp) for specimen Preston B2-2L. Rate of heating was 10 °C/min. Type of model was the Simmons with 6 pseudo-reactions.

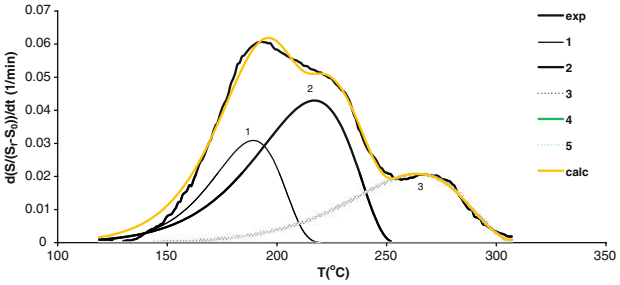

Fig. 9. Example of model fitting (calc) to data (exp) for specimen Iwata 1. Rate of heating was 5 °C/min. Type of model was $f(S) = S^n$ (Nightingale) 6 Reactions.

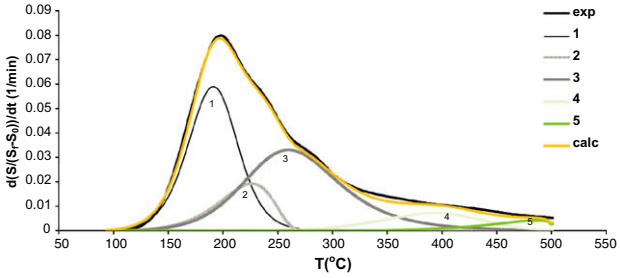

Fig. 10. Example of model fitting (calc) to data (exp) for Preston B12-2L. Rate of heating was 10 °C/min. Type of model was $f(S) = S^n$ (Nightingale) 5 Reactions. The convergence between experimental and calculated values is almost identical. The shape of the predicted curve is a good fit to the experimental.

In Fig. 11 the DSC profile of specimen Iwata 5 is shown. The DSC profile of the experimental curve is compared with the calculated curve, along with the pseudo reactions used to construct the calculated curve. The DSC profiles are a plot of the time derivative of the normalized activation energy versus time. The rate of heating in this case was 5 °C/min. The type of model used is $f(S) = S^n$ (Nightingale – 5 reactions). The DSC profile of the Iwata series of experiments are different compared to the Preston and the Simmons results, possibly because of the differences of the type of the graphite or irradiation conditions. Despite this, the application of the predictive model used for the Preston and Simmons series of DSC data, gives very good results when applied to the Iwata series. Excellent convergence is obtained between experimental and calculated results and the shape of the calculated curve closely follows the experimental data. The participation of 4th and 5th reactions is almost zero for the Iwata series.

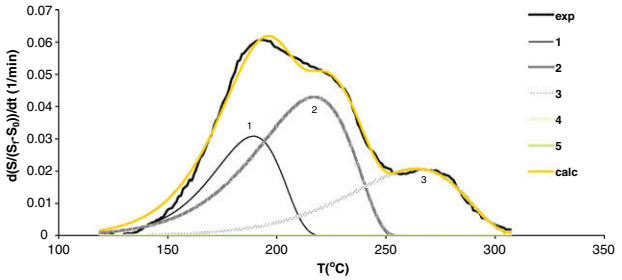

Fig. 11. Example of model fitting (calc) to data (exp) for specimen Iwata 5. Rate of heating was 5 °C/min. Type of model used was $f(S) = S^n$ (Nightingale) 5 Reactions. The DSC profile of the Iwata series of experiments is relatively different compared to the Simmons and the Preston curve, probably due to the differences of the type of graphite. Despite this the application of the calculated model derived for the Simmons and Preston series of DSC data, gives very good results when applied to the Iwata series. The participation of 4th and 5th reactions is almost zero for the Iwata series.

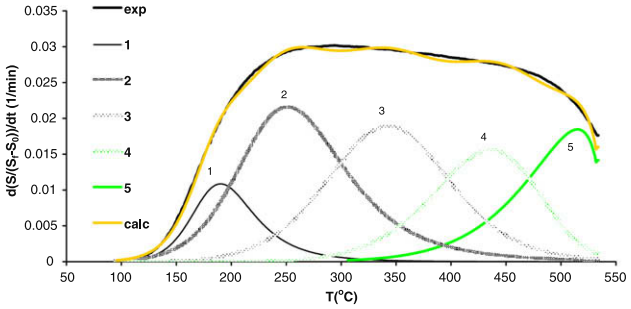

Fig. 12. Example of model fitting (calc) to data (exp) for specimen Lexa f. Rate of heating was 10 °C/min. Type of model used was $f(S) = S^n$ (Nightingale) 5 Reactions. The DSC profile of the Lexa f and g samples is relatively different compared with all the other DSC profiles probably because of the differences in irradiation dose. Despite that the application of the calculated model derived for the Simmons and Preston series of DSC data, gives very good results when applied to the Lexa f and g profiles.

In Fig. 12 the DSC profile of specimen Lexa f. is shown. The DSC profile of the experimental curve is compared with the calculated curve, along with the pseudo reactions used to construct the calculated curve. The DSC profiles are a plot of the time derivative of the normalized energy released versus time. The rate of heating in this case in this case was 10 °C/min. The type of model used was $f(S) = S^n$ (Nightingale – 5 reactions). The DSC profile of the Lexa f. and g. samples are relatively different compared with all the other DSC profiles possibly because of the differences in irradiation dose. Fig. 10 shows that application of the predictive model, originally derived for the Preston and Simmons series of DSC data, gives very good results when applied to the Lexa f and g profiles. Excellent convergence between experimental and calculated values is obtained and the shape of the calculated curve closely follows the experimental results despite the differences in the DSC shapes.

8. General discussion

In Table 2 a comparison between the three models tested for all the series of experimental data is given. It can be concluded is that the $f(S) = S^n$ (Nightingale – 5 reaction) model is the most effective, in terms of achieving good convergence for all the series of data. The model that converges best is the Nightingale $f(S) = S^n$ 5 – reaction model as all the results derive a *Dev1* of less than 3%, and there is a good match between the experimental and predicted curves.

Table 2
Comparison between the three models tested for all the series of data [1–4]

DSC DATA	6 reactions $f(S) = S$ (Simmons) (*Dev1%*)	6 reactions. $f(S) = S^n$ (Nightingale) (*Dev1%*)	5 reactions. $f(S) = S^n$ (Nightingale) (*Dev1%*)
Iwata 1	3.99	2.09	1.08
Iwata 2	6.01	4.07	1.80
Iwata 5	6.75	4.69	2.67
Iwata 10	5.53	3.90	1.85
Iwata 20	6.31	4.98	2.66
Iwata 50	5.77	4.45	2.67
Iwata 100	6.57	5.86	2.80
Lexa a	2.46	1.68	1.20
Lexa b	3.18	2.25	1.03
Lexa c	2.60	1.79	0.61
Lexa d	1.69	1.54	0.48
Lexa d	1.11	1.00	1.57
Lexa e	8.02	1.43	1.64
Lexa g	1.91	1.32	0.75
B2-2L Preston	1.78	1.48	1.42
B2-12L Preston	2.29	1.94	0.64
TMS 2 33-57-15 BR	2.90	2.04	1.23
W/Scale 2,5	2.31	2.01	1.31
W/Scale 2,5 II	2.34	2.01	1.55
W/Scale 25	3.12	2.57	1.16
W/Scale 25 II	3.29	2.67	1.23
W/Scale 50	3.47	2.91	1.42

The Nightingale $f(S) = S^n$ 5 – reaction model (Table 2) gives the closest results. In examining the stability of the values from the different models it may be expected that the values of A and E_a will have little variation, but that the values of n and c may vary more extensively owing to the different experimental conditions and irradiation fluence and the different types of graphite (slight differences in crystallinity). The irradiation history need also to be considered, since some of the specimens were irradiated in production reactors while others have been irradiated for shorter periods of times in Material Test Reactors.

By examining the results for the first reaction presented in Tables 3 and 4, the stability of A and E_a are similar in all cases whereas n and c vary. The values of A and E_a in the second reaction vary more that for the first reaction although the activation energies are of the same order around 77 kJ/mol. The values of A in the third reaction mainly vary between 5.34×10^6 and 8.39×10^6 reaching 3.18×10^7 at some of the high rates in the Iwata series, the activation energy is around 75 kJ/mol varying between 65 and 85. The fourth reaction was not required when modelling the Iwata series. The value of A where has a value of 1.88×10^6 in most cases. In the fourth series A remains mainly around 5.07×10^5 for the Lexa f and Lexa g specimens. The fifth reaction, also absent in the Iwata series, gives a value for A between 2.47×10^5 or 2.88×10^5, with Activation energies around 75 kJ/mol ranging between 70 and 90.

The values of n and c (Tables 3 and 4) for the different DSC runs show more variation. The factor of n is generally increasing for the first two reactions and decreasing for the other three reactions, with increased irradiation fluence, as can be assessed from the Lexa model results. The heating rate appears to have some affect on n since there is an obvious increase in n with increasing heating rate for the first reaction. The factor c is a measure of the types of defect reactions in the overall annealing process. The factor c does not indicate the percentage of different types of defects on the overall defect population but the part with which they contribute to the

Table 3
Overall results for Nightingale $f(S) = S^n$, model with 5 pseudo-reactions

Reactions		1st				2nd				3rd				4th				5th			
	Rate (°C/min)	A (1/min)	E_a (kJ/mol)	n	c (%)	A (1/min)	E_a (kJ/mol)	n	c (%)	A (1/min)	E_a (kJ/mol)	n	c(%)	A (1/min)	E_a (kJ/mol)	n	c (%)	A (1/min)	E_a (kJ/mol)	n	c (%)
Iwata 1	1	7.04×10^{10}	103	0.99	32.4	1.55×10^{7}	77	0.88	49.3	5.47×10^{6}	82	0.76	23.3	–	–	–	–	–	–	–	–
Iwata 2	2	7.04×10^{10}	103	0.90	31.0	1.55×10^{7}	76	0.79	51.6	5.47×10^{6}	81	0.70	22.4	–	–	–	–	–	–	–	–
Iwata 5	5	7.04×10^{10}	102	0.85	28.6	2.35×10^{7}	76	0.76	52.8	8.56×10^{6}	80	0.81	30.1	–	–	–	–	–	–	–	–
Iwata 10	10	7.04×10^{10}	100	0.87	25.6	2.35×10^{7}	75	0.77	53.1	8.56×10^{6}	78	0.74	30.8	–	–	–	–	–	–	–	–
Iwata 20	20	7.04×10^{10}	102	1.91	71.3	2.35×10^{7}	75	0.47	14.9	8.56×10^{6}	77	0.68	25.2	–	–	–	–	–	–	–	–
Iwata 50	50	7.04×10^{10}	101	1.49	48.6	6.63×10^{7}	77	0.51	20.2	3.18×10^{7}	80	0.88	36.2	–	–	–	–	–	–	–	–
Iwata 100	100	7.04×10^{10}	100	1.57	48.1	6.63×10^{7}	76	0.46	19.8	3.18×10^{7}	78	0.85	37.0	–	–	–	–	–	–	–	–
Lexa a	10	7.04×10^{10}	97	0.98	11.7	1.55×10^{7}	70	0.99	22.9	5.47×10^{6}	75	2.01	33.0	1.88×10^{6}	89	1.55	22.4	2.87×10^{5}	93	0.39	10.0
Lexa b	10	7.04×10^{10}	97	1.00	24.5	1.55×10^{7}	71	0.79	25.4	5.47×10^{6}	74	1.28	32.5	1.88×10^{6}	83	0.95	8.3	2.87×10^{5}	83	0.87	9.3
Lexa c	10	7.04×10^{10}	97	1.05	20.7	1.55×10^{7}	71	0.87	23.6	5.47×10^{6}	73	1.50	33.7	1.88×10^{6}	84	1.58	12.2	2.87×10^{5}	88	0.95	9.9
Lexa d	10	7.04×10^{10}	97	1.32	16.8	1.55×10^{7}	71	1.13	30.2	5.47×10^{6}	75	1.99	30.2	1.88×10^{6}	87	1.48	14.2	2.87×10^{5}	90	0.69	8.6
Lexa e	10	7.04×10^{10}	96	0.99	6.2	1.55×10^{7}	70	1.58	48.8	5.47×10^{6}	76	1.99	24.3	1.88×10^{6}	87	1.46	12.5	2.87×10^{5}	90	0.72	8.1
Lexa f	10	7.04×10^{10}	99	2.52	9.5	8.86×10^{5}	66	2.17	30.3	8.39×10^{4}	67	1.55	28.7	5.07×10^{5}	87	1.12	20.2	2.47×10^{5}	92	0.35	16.7
Lexa g	10	7.04×10^{10}	95	3.59	15.6	8.86×10^{5}	64	2.29	26.2	8.39×10^{4}	65	1.66	29.6	5.07×10^{5}	87	1.16	19.0	2.47×10^{5}	92	0.33	14.9
PRESTON B2-2L	10	7.04×10^{10}	98	1.26	20.5	1.55×10^{7}	71	1.36	40.6	5.47×10^{6}	75	1.92	35.6	1.88×10^{6}	88	1.24	6.1	2.87×10^{5}	90	0.18	2.5
PRESTON B12-2L	10	7.04×10^{10}	99	1.60	39.2	1.55×10^{7}	73	0.81	13.1	5.478×10^{6}	75	2.03	41.0	1.88×10^{6}	88	1.24	8.8	2.87×10^{5}	90	0.21	3.2
TMR 2 33-57-15 BR	10	7.04×10^{10}	95	1.99	14.3	1.55×10^{7}	72	2.54	45.1	5.47×10^{6}	84	2.30	18.8	1.88×10^{6}	113	0.52	8.5	2.87×10^{5}	84	1.61	18.6
Windscale 2.5	2.5	7.04×10^{10}	103	1.79	28.7	1.55×10^{7}	77	1.22	21.4	5.47×10^{6}	82	2.21	26.7	1.87×10^{6}	109	0.65	10.0	2.87×10^{5}	83	1.59	18.6
Windscale 2.5 II	2.5	7.04×10^{10}	103	1.79	28.7	1.55×10^{7}	77	1.22	21.4	5.47×10^{6}	82	2.21	26.7	1.87×10^{6}	109	0.65	10.0	2.87×10^{5}	83	1.59	18.6
Windscale 25	25	7.04×10^{10}	102	2.02	46.0	1.55×10^{7}	73	0.69	4.5	5.47×10^{6}	74	1.61	23.1	1.87×10^{6}	96	0.38	10.3	2.88×10^{5}	73	1.28	21.6
Windscale 25 II	25	7.048×10^{10}	102	2.02	46.0	1.558×10^{7}	74	0.69	4.5	5.478×10^{6}	75	1.61	23.1	1.87×10^{6}	97	0.38	10.3	2.88×10^{5}	74	1.28	21.6
Windscale 50	50	7.04×10^{10}	102	2.02	46.0	1.55×10^{7}	72	0.69	4.5	5.47×10^{6}	74	1.61	23.1	1.87×10^{6}	94	0.38	10.3	2.88×10^{5}	70	1.28	21.6

Table 4
Variation of assessed values for the Nightingale $f(S) = S^n$ model with 5 pseudo-reactions

	A (1/min)	E (kJ/mol)	n	c (%)
1st Reaction				
Min	7.04×10^{10}	95	0.85	6.20
Max	7.04×10^{10}	103	3.59	71.30
Mean	7.04×10^{10}	100	1.57	30.00
2nd Reaction				
Min	8.86×10^{5}	64	0.46	4.50
Max	6.63×10^{7}	77	2.54	53.10
Mean	1.99×10^{7}	73	1.08	26.13
3rd Reaction				
Min	8.39×10^{4}	66	0.68	18.80
Max	3.18×10^{7}	84	2.30	41.00
Mean	7.80×10^{6}	76	1.50	28.87
4th Reaction				
Min	5.07×10^{5}	83	0.38	6.10
Max	1.88×10^{6}	113	1.58	22.40
Mean	1.69×10^{6}	93	0.98	12.21
5th Reaction				
Min	2.47×10^{5}	70	0.18	2.50
Max	2.88×10^{5}	93	1.61	21.60
Mean	2.82×10^{5}	85	0.90	13.59

A – Little variation in most of the reactions. E_a – Little variation and a range of 20 kJ/mol between the mean. n, c – Extended variations probably due to different experimental conditions (heating rate, irradiation dose) or types of graphite.

energy released when annealed. That implies that some types of defects do not contribute their full capacity to the overall energy released when the irradiation for different values of fluence or even when the heating rate changes.

9. Conclusions

- The independent parallel reactions model had been shown to be able to describe the annealing kinetics of stored energy in irradiated graphite. In particular a model proposed by Nightingale with 5 pseudo reactions, was able to give good quality fits to stored energy data made on samples for polycrystalline nuclear graphite originating from different types of coke, manufacture process and irradiation histories.
- The variation in the predicted model parameters A, E_a, n and c for each of the five reactions were of similar order for all the grades of graphite investigated (with the exception that the 4th and 5th order terms were not required for the Iawa data.
- The differences in the parameters can probably be explained by the variety of graphite examined as well as the differences in the irradiation and experimental conditions. However, despite these differences, a relative stability model has been achieved.

Acknowledgements

The authors would like to acknowledge the Greek State Scholarships Foundation for financial support, and Dr Stephen Preston for provision of part of the experimental data.

References

[1] S.D.Preston, Preliminary measurements of stored energy in graphite dowels from the Windscale piles, Industrial Report, Nirex, AEA Technology, September 1997 (Downgraded to unclassified on 4/2/2004).
[2] J.H.W. Simmons, Stored Energy in the Windscale Piles, AEA RS 5283, AEA Technology, March 1994.
[3] Dusan Lexa, A. Jeremy Kropf, J. Nucl. Mater. 348 (2006) 122.
[4] Tadao Iwata, J. Nucl. Mater. 133&134 (1985) 361.
[5] R.E. Nightingale, in: TID-7565(Pt. 1) US/UK Graphite Conference St., Giles Court, London, December 1957.
[6] Gabor Varhegyi, J. Anal. Appl. Pyrol. 79 (2007) 278.
[7] L. Sorum, M.G. Gronli, J.E. Hustad, Fuel 80 (2001) 217.
[8] A.A. Joraid, Phys. B: Cond. Matter. (2006) 263.
[9] Gábor Várhegyi, Piroska Szabó, Emma Jakab, Ferenc Till, J. Anal. Appl. Pyrol. 57 (2) (2001) 203.
[10] L. Sørum, M.G. Grønli, J.E. Hustad, Fuel 80 (9) (2001) 1217.
[11] Gábor Várhegyi, Ferenc Till, Thermochimica Acta 329 (2) (1999) 141.
[12] D. Vamvuka, E. Kakaras, E. Kastanaki, P. Grammelis, Fuel 82 (15–17) (2003) 1949.
[13] Eleni Kastanaki, Despina Vamvuka, Fuel 85 (9) (2006) 1186.